



Published in final edited form as:

*Clin Radiol.* 2019 January ; 74(1): 29–36. doi:10.1016/j.crad.2017.12.003.

## Advances in non-contrast quiescent-interval slice-selective (QISS) magnetic resonance angiography

R. R. Edelman<sup>1,2,\*</sup>, M. Carr<sup>2</sup>, and I. Kocktzoglou<sup>2,3</sup>

<sup>1</sup>Radiology, Northwestern Memorial Hospital, Chicago, IL, USA

<sup>2</sup>Radiology, Northshore University HealthSystem, Evanston, IL, USA

<sup>3</sup>Radiology, University of Chicago Pritzker School of Medicine, Chicago, IL, USA

### Abstract

There is a pressing clinical need to develop accurate, efficient non-contrast magnetic resonance angiography (NC-MRA) techniques. Our efforts in the field have focused on a novel non-subtractive technique called quiescent-interval slice-selective (QISS) MRA. Compared with other NC-MRA techniques, QISS has the advantage of being more accurate while enabling a simpler and more efficient workflow. The original implementation, which uses electrocardiogram (ECG) gating and a Cartesian k-space trajectory, is a reliable technique for the evaluation of peripheral arterial disease (PAD). Recent advances in QISS technology include the use of a radial k-space trajectory, which facilitates rapid imaging of the coronary, renal, and pulmonary arteries as well as other vascular beds, and ungated (“UnQISS”) acquisitions for PAD.

### INTRODUCTION

Peripheral arterial disease (PAD) is a potentially debilitating manifestation of systemic atherosclerosis affecting more than 200 million people worldwide.<sup>1,2</sup> Over the last decade, the incidence of PAD has risen globally by approximately 13% in high-income countries and 29% in low-income countries.<sup>3</sup> Patients with PAD have a 10-year risk of death of 40%, a threefold higher risk of all-cause death, and sixfold higher risk of cardiovascular-related death than patients without PAD.<sup>4</sup> It is associated with an increased risk of myocardial infarction, stroke, and cardiovascular-related mortality.<sup>1,2</sup> Diabetes and smoking are the strongest risk factors for PAD. Accurate diagnosis is essential for managing the disease and confers useful prognostic information.

The availability of accurate non-invasive imaging tests has decreased the need for preoperative digital subtraction angiography (DSA) in the evaluation of PAD. The ankle brachial index (ABI) is an excellent screening test for haemodynamically significant PAD

\*Guarantor and correspondent: R. R. Edelman, Walgreen Building, G534, 2650 Ridge Avenue, Evanston, IL 60201, USA. Tel.: (847) 570-2098, address redelman999@gmail.com.

**Publisher's Disclaimer:** This is a PDF file of an unedited manuscript that has been accepted for publication. As a service to our customers we are providing this early version of the manuscript. The manuscript will undergo copyediting, typesetting, and review of the resulting proof before it is published in its final citable form. Please note that during the production process errors may be discovered which could affect the content, and all legal disclaimers that apply to the journal pertain.

and can be performed in conjunction with Doppler waveform analysis and segmental pressure measurement to increase accuracy;<sup>5</sup> however, its sensitivity is low in elderly patients and those with diabetes.<sup>6</sup> Computed tomography angiography (CTA) offers high spatial resolution and short scan times without the risks associated with DSA, and is generally accurate for PAD.<sup>7,8</sup> CTA is often acquired to provide a vascular roadmap prior to percutaneous interventional procedures; however, the clinical utility of CTA is diminished by the presence of vessel wall calcifications, associated with diabetes, heart disease, and advanced age, which cause blooming artefacts that obscure the vessel lumen.<sup>9</sup> CTA has the further disadvantages of exposing patients to ionising radiation and the risk of contrast-induced nephropathy (CIN), which is of particular concern because nearly 40% of patients with PAD have significant renal dysfunction.<sup>10</sup> Contrast-enhanced magnetic resonance angiography (CEMRA) has also been shown to be highly accurate for the detection of stenoses 50% within the lower extremity arterial tree.<sup>11,12,13</sup> Unfortunately, the administration of gadolinium-based contrast agents in patients with severely impaired renal function is contraindicated due to the risk of nephrogenic systemic fibrosis (NSF).<sup>14</sup> Moreover, there is growing concern about the accumulation of gadolinium chelates within the brain, the long-term consequences of which are unknown.<sup>15</sup> This concern is exacerbated by the use of relatively high gadolinium doses for peripheral CEMRA, as well as by the potential cumulative impact when these patients have multiple CEMRA examinations during their lifetime. The use of contrast agents also increases study cost and necessitates inconvenient point-of-service renal function testing. Given these safety concerns, along with the potential cost savings involved in eliminating the need to administer a contrast agent, there is a pressing need to develop efficient non-contrast (NC)-MRA techniques that can match the accuracy of CEMRA.

## EXISTING TECHNOLOGY FOR NC-MRA

Techniques for NC-MRA include electrocardiographic (ECG)-gated subtractive three-dimensional (3D) fast spin-echo (FSE) imaging such as fresh blood imaging (FBI)<sup>16</sup> and NATIVE SPACE (NATIVE = Non-contrast Angiography of the Arteries and Veins; SPACE = Sampling Perfection with Application Optimised Contrast by using different flip angle Evolution), as well as variants predicated on 3D steady-state free precession (bSSFP), such as flow-sensitive dephasing.<sup>17</sup> The use of image subtraction in conjunction with a time-consuming 3D acquisition makes all these techniques highly sensitive to misregistration artefact from patient motion, which is common in elderly patients who often suffer from back pain or restless legs. The problem of misregistration is particularly severe in the abdominal and pelvic regions due to breathing and bowel peristalsis. Along with the problem of misregistration, these techniques may exaggerate the severity of disease whenever the flow-sensitising gradient or the timing of the acquisition with respect to the arterial pulse wave is suboptimal. In one report using an FBI-based approach, nearly 50% of studies were non-diagnostic due to artefacts.<sup>18</sup> Although these techniques remain promising and are under active development, none has yet proved reliable for whole-leg studies in routine clinical usage, and there is a paucity of clinical validation through multicentre trials.

## QUIESCENT-INTERVAL SLICE-SELECTIVE (QISS) MRA

Over the last several years, our efforts in the field of NC-MRA have focused on a novel non-subtractive technique called QISS MRA (Fig. 1).<sup>19</sup> Compared with subtractive approaches such as FBI and NATIVE SPACE, QISS has several advantages.<sup>20</sup> The use of a single-shot acquisition with a very short (200–300 msec) period of data collection for each slice helps to minimise the sensitivity to patient motion compared with lengthier subtractive 3D NC-MRA techniques, where any motion during the several-minute scan may cause artefacts. Breath-holding (not practical with a subtractive 3D acquisition) can be used with QISS in the upper pelvis and abdomen to avoid respiratory artefact. Perhaps the greatest advantage is that QISS, by design, is a “push-button” technique with no need to acquire scout images, timing scans, or to make patient-specific adjustments to the imaging parameters. As a consequence, it is easy and efficient for the technologist to set up and run.

QISS has proven to be highly accurate in multiple clinical trials at both 1.5 and 3 T.<sup>21,22,23,24,25,26,27</sup> Consequently, QISS has become a useful alternative to CEMRA and CTA, particularly in patients who have impaired renal function. In diabetic patients, QISS avoids image artefacts seen with CTA from small vessel calcifications (Fig. 2).<sup>28</sup> If desired, peripheral vascular calcifications that are unapparent with QISS MRA can be accurately visualised through the acquisition of a separate proton density-weighted, in-phase stack of stars pulse sequence.<sup>29</sup>

### Ungated QISS (UnQISS)

Compared with CTA and CEMRA, one of the potential drawbacks of QISS is its dependence on cardiac gating. Although not a concern in the majority of patients, some individuals with PAD suffer from arrhythmias that may cause artefacts on the QISS MRA. Another concern is magnetohydrodynamic interference at 3 T, which occasionally makes it difficult to obtain a reliable ECG tracing. In this subgroup of patients, none of the existing NC-MRA techniques, including FBI, flow-sensitive dephasing, QISS, or even ECG-triggered time-of-flight MRA are expected to provide diagnostic results. We therefore developed a QISS variant, which we call “UnQISS” (Figs. 3 and 4), that eliminates the need for ECG gating.<sup>30</sup> Without ECG or pulse gating, data are acquired at random phases of the cardiac cycle. For some slices, data are acquired during periods of slow diastolic flow whereas for other slices, data are acquired during periods of rapid systolic flow. Unfortunately, the bSSFP readout is prone to severe artefacts when data are acquired during rapid flow.<sup>31</sup> In order to overcome this limitation, recent implementations of UnQISS read out the MR signal using a novel variant on bSSFP called “fast interrupted steady-state” (FISS).<sup>32</sup> FISS is a recently described technique in which the bSSFP readout is interrupted and spoiled at frequent intervals and data are acquired using a radial instead of a Cartesian readout. Scan time for UnQISS is about twice that for QISS, due to the need for a much longer inflow time (>1 second for UnQISS versus <300 ms for QISS), which prolongs the sequence repetition time (TR). Because of the long inflow time, a tracking inversion RF pulse is used instead of a tracking saturation RF pulse to better suppress signal from venous spins. The UnQISS technique can also be used to produce high-quality peripheral venograms. In this case, the tracking

inversion is placed above the slice to suppress inflowing arterial spins, instead of below the slice.

### Susceptibility artefacts

QISS uses a bSSFP pulse sequence to read out the data because of its high efficiency, signal-to-noise ratio (SNR), and intrinsic flow compensation; however, the bSSFP readout can result in severe magnetic susceptibility-related artefacts in patients with hip replacements, much worse than those seen with CEMRA. These artefacts can be greatly reduced by the use of a fast low angle shot (FLASH) readout instead of bSSFP, at the expense of lower SNR and greater flow saturation (Fig. 5).

### Second-Generation QISS Techniques

The original QISS technique used a Cartesian k-space trajectory; however, for clinical applications of QISS outside of the peripheral vasculature, the use of a radial k-space trajectory offers major benefits. Radial QISS has the advantages of greatly reduced motion sensitivity<sup>33</sup>, more flexible control over temporal and spatial resolution, and support for higher undersampling factors compared with a standard Cartesian implementation. Using a Cartesian trajectory, scan time is reduced by decreasing the number of phase-encodes, which results in an undesirable decrease in spatial resolution. Alternatively, one can image faster by using parallel imaging techniques;<sup>34</sup> however, high parallel acceleration factors cause an unacceptable increase in image noise due to spatially-dependent “geometry factor” effects. Unlike a Cartesian acquisition, spatial resolution is not degraded with a radial acquisition as the number of views is decreased so long as radial streak artefacts can be adequately suppressed. With radial QISS, streak artefacts are minimised by the suppression of background signal intensity, which is achieved through the combination of fat saturation and in-plane spatial saturation. Streak artefacts are further suppressed by sampling k-space using equidistant azimuthal view angles. With these modifications, radial QISS allows the use of higher scan accelerations than is practical with a Cartesian acquisition.

Radial QISS can be used to image the coronary arteries<sup>35</sup>, where it provides a breath-hold alternative to lengthier free-breathing, navigator-gated 3D techniques.<sup>36</sup> For coronary imaging, radial QISS is typically acquired with two or three shots to keep temporal resolution to about 150 ms or less; this is usually sufficient to minimise artefacts from coronary motion so long as data are collected during mid to end diastole (Fig. 6). Although still in the early stages of development, potential clinical applications include localisation of the vessel origins in patients with suspected coronary anomalies and the evaluation of coronary artery disease.

In situations where very high temporal resolution is not required, such as for imaging of the renal, mesenteric or pulmonary arteries, a single-shot radial QISS acquisition allows for efficient breath-hold coverage of a vascular territory with high SNR and arterial-to-background contrast (Fig. 7).

Pulmonary embolism is a potentially lethal condition that is usually evaluated by CTA.<sup>37</sup> Alternatively, a contrast-enhanced MRA protocol has shown potential utility for diagnosis.<sup>38</sup> In certain patient groups, however, neither technique is entirely satisfactory. For instance, in

pregnant patients, there is concern about exposing the fetus to ionising radiation with CTA, while gadolinium-based contrast agents are contraindicated. In patients with poor renal function, iodinated and gadolinium-based contrast agents should be avoided. A recent study using a single-shot, radial implementation of QISS MRA has shown promise for rapidly depicting the pulmonary arterial anatomy and can detect pulmonary embolism.<sup>39</sup> Both breath-hold and navigator-gated acquisitions are feasible (Fig. 8). Further work is needed to determine the accuracy of this technique.

Perhaps the biggest eventual application of QISS will be for the evaluation of the cerebrovascular system and extracranial carotid arteries.<sup>40,41</sup> The most recent version of this technique uses an ungated radial QISS acquisition with a fast-low angle shot (FLASH) readout. It can produce images that rival the quality of CEMRA and greatly surpass the quality of time-of-flight MRA techniques that are still in widespread use (Fig. 9).

## CONCLUSIONS

QISS MRA has already proven to be a valuable alternative to CTA and CEMRA for the evaluation of the peripheral vasculature in patients with suspected PAD, particularly in the setting of impaired renal function. Given the technique's high accuracy and the cost savings involved in eliminating contrast agent administration, QISS provides a viable alternative to CEMRA even in patients with normal renal function. With ongoing technical advances, such as the use of radial k-space trajectories and advanced image processing advances such as compressed sensing<sup>42</sup>, it may eventually prove to be a useful diagnostic tool for a wide range of vascular disorders.

## Acknowledgments

This study was funded by NIH grants R01 HL130093, R21 HL126015, and R01 HL137920.

## References

1. Leng GC, Lee AJ, Fowkes FG, et al. Incidence, natural history and cardiovascular events in symptomatic and asymptomatic peripheral arterial disease in the general population. *Int J Epidemiol.* 1996; 25:1172–1181. [PubMed: 9027521]
2. Selvin E, Erlinger TP. Prevalence of and risk factors for peripheral arterial disease in the United States: results from the National Health and Nutrition Examination Survey, 1999–2000. *Circulation.* 2004; 110:738–743. [PubMed: 15262830]
3. Hirsch AT, Duval S. The global pandemic of peripheral artery disease. *Lancet.* 2013 Oct 19; 382(9901):1312–4. DOI: 10.1016/S0140-6736(13)61576-7 [PubMed: 23915884]
4. Arain FA, Cooper LT. Peripheral arterial disease: diagnosis and management. *Mayo Clin Proc.* 2008; 83:944–950. [PubMed: 18674479]
5. Hirsch AT, Haskal ZJ, Hertzler NR, et al. ACC/AHA 2005 Practice Guidelines for the Management of Patients With Peripheral Arterial Disease (Lower Extremity, Renal, Mesenteric, and Abdominal Aortic). *JACC.* 2006; 47:1239–1312. [PubMed: 16545667]
6. Xu D, Li J, Zou L, Xu Y, Hu D, Pagoto SL, Ma Y. Sensitivity and specificity of the ankle—brachial index to diagnose peripheral artery disease: a structured review. *Vasc Med.* 2010; 15:361–369. [PubMed: 20926495]
7. Hessel SJ, Adams DF, Abrams HL. Complications of angiography. *Radiology.* 1981; 138:273–281. [PubMed: 7455105]

8. Catalano C, Fraioli F, Laghi A, et al. Infrarenal aortic and lower-extremity arterial disease: diagnostic performance of multi-detector row CT angiography. *Radiology*. 2004; 231:555–563. [PubMed: 15128997]
9. Ouwendijk R, Kock MC, van Dijk LC, van Sambeek MR, Stijnen T, Hunink MG. Vessel wall calcifications at multi-detector row CT angiography in patients with peripheral arterial disease: effect on clinical utility and clinical predictors. *Radiology*. 2006; 241:603–608. [PubMed: 16966479]
10. Tranche-Iparraguirre S, Marín-Iranzo R, Fernández-de Sanmamed R, Riesgo-García A, Hevia-Rodríguez E, García-Casas JB. Peripheral arterial disease and kidney failure: a frequent association. *Nefrologia*. 2012 May 14; 32(3):313–20. DOI: 10.3265/Nefrologia.pre2011.Nov.11172 [PubMed: 22508143]
11. Menke J, Larsen J. Meta-analysis: accuracy of contrast-enhanced magnetic resonance angiography for assessing steno-occlusions in peripheral arterial disease. *Ann Intern Med*. 2010; 153:325–334. [PubMed: 20820041]
12. Baum RA, Rutter CM, Sunshine JH, et al. Multicenter trial to evaluate vascular magnetic resonance angiography of the lower extremity. American College of Radiology Rapid Technology Assessment Group. *JAMA*. 1995; 274:875–880. [PubMed: 7674500]
13. Koelemay MJ, Lijmer JG, Stoker J, Legemate DA, Bossuyt PM. Magnetic resonance angiography for the evaluation of lower extremity arterial disease: a meta-analysis. *JAMA*. 2001; 285:1338–1345. [PubMed: 11255390]
14. Prince MR, Zhang H, Morris M, et al. Incidence of nephrogenic systemic fibrosis at two large medical centers. *Radiology*. 2008; 248:807–816. [PubMed: 18710976]
15. Olchoway C, Cebulski K, Łasecki M, et al. The presence of the gadolinium-based contrast agent depositions in the brain and symptoms of gadolinium neurotoxicity — a systematic review. *PLoS ONE*. 2017; 12(2):e0171704.doi: 10.1371/journal.pone.0171704 [PubMed: 28187173]
16. Miyazaki M, Takai H, Sugiura S, Wada H, Kuwahara R, Urata J. Peripheral MR angiography: separation of arteries from veins with flow-spoiled gradient pulses in electrocardiography-triggered three-dimensional half-Fourier fast spin-echo imaging. *Radiology*. 2003; 227:890–896. [PubMed: 12702824]
17. Fan Z, Sheehan J, Bi X, Liu X, Carr J, Li D, et al. 3D noncontrast MR angiography of the distal lower extremities using flow-sensitive dephasing (FSD)-prepared balanced SSFP. *Magn Reson Med*. 2009; 62:1523–1532. [PubMed: 19877278]
18. Lim RP, Hecht EM, Xu J, Babb JS, et al. 3D nongadolinium-enhanced ECG-gated MRA of the distal lower extremities: preliminary clinical experience. *J Magn Reson Imag*. 2008; 28:181–189.
19. Edelman RR, Sheehan JJ, Dunkle E, Schindler N, Carr J, Koktzoglou I. Quiescent-interval single-shot unenhanced magnetic resonance angiography of peripheral vascular disease: technical considerations and clinical feasibility. *Magn Reson Med*. 2010; 63:951–958. [PubMed: 20373396]
20. Ward EV, Galizia MS, Usman A, Popescu AR, Dunkle E, Edelman RR. Comparison of quiescent inflow single-shot and native space for nonenhanced peripheral MR angiography. *J Magn Reson Imaging*. 2013; 38(6):1531–1538. DOI: 10.1002/jmri.24124 [PubMed: 23564638]
21. Hodnett PA, Koktzoglou I, Davarpanah AH, et al. Evaluation of peripheral arterial disease with nonenhanced quiescent-interval single shot MR angiography. *Radiology*. 2011; 260:282–293. [PubMed: 21502384]
22. Klasen J, Blondin D, Schmitt P, et al. Nonenhanced ECG-gated quiescent-interval single-shot MRA (QISS-MRA) of the lower extremities: comparison with contrast-enhanced MRA. *Clin Radiol*. 2012; 67:441–446. [PubMed: 22142498]
23. Hansmann J, Morelli JN, Michaely HJ, Riester T, Budjan J, Schoenberg SO, Attenberger UI. Nonenhanced ECG-gated quiescent-interval single shot MRA: image quality and stenosis assessment at 3 tesla compared with contrast-enhanced MRA and digital subtraction angiography. *J Magn Reson Imaging*. 2014; 39:1486–1493. DOI: 10.1002/jmri.24324 [PubMed: 24338813]
24. Knobloch G, Gielen M, Lauff MT, et al. ECG-gated quiescent-interval single-shot MR angiography of the lower extremities: initial experience at 3 T. *Clin Radiol*. 2014; 69(5):485–491. [PubMed: 24613581]

25. Thierfelder KM, Meimarakis G, Nikolaou K, et al. Non-contrast-enhanced MR angiography at 3 Tesla in patients with advanced peripheral arterial occlusive disease. *PLoS One*. 2014; 9(3):e91078. [PubMed: 24608937]
26. Amin P, Collins JD, Koktzoglou I, et al. Evaluating peripheral arterial disease with unenhanced quiescent-interval single-shot MR angiography at 3 T. *AJR Am J Roentgenol*. 2014; 202(4):886–893. DOI: 10.2214/AJR.13.11243 [PubMed: 24660721]
27. Mustafa MA, Jaskolka JJ, Tan K, et al. Non-contrast-enhanced MR angiography in critical limb ischemia: performance of quiescent-interval single-shot (QISS) and TSE-based subtraction techniques. *Eur Radiol*. 2017; 27:1218–1226. [PubMed: 27352087]
28. Hodnett PA, Ward EV, Davarpanah AH, et al. Peripheral arterial disease in a symptomatic diabetic population: prospective comparison of rapid unenhanced MR angiography (MRA) with contrast-enhanced MRA. *AJR Am J Roentgenol*. 2011; 197:1466–73. DOI: 10.2214/AJR.10.6091 [PubMed: 22109304]
29. Ferreira Botelho MP, Koktzoglou I, Collins JD, et al. MR imaging of iliofemoral peripheral vascular calcifications using proton density-weighted, in-phase three-dimensional stack-of-stars gradient echo. *Magn Reson Med*. 2017 Jun; 77(6):2146–2152. DOI: 10.1002/mrm.26295 [PubMed: 27297954]
30. Edelman RR, Giri S, Murphy IG, Flanagan O, Speier P, Koktzoglou I. Ungated radial quiescent-inflow single-shot (UnQISS) magnetic resonance angiography using optimized azimuthal equidistant projections. *Magn Reson Med*. 2014; 72:1522–1529. [PubMed: 25257379]
31. Markl M, Alley MT, Elkins CJ, Pelc NJ. Flow effects in balanced steady state free precession imaging. *Magn Reson Med*. 2003 Nov; 50(5):892–903. [PubMed: 14586999]
32. Koktzoglou I, Edelman RR. Radial fast interrupted steady-state (FISS) magnetic resonance imaging. *Magn Reson Med*. 2017 Aug 30. doi: 10.1002/mrm.26881
33. Glover GH, Pauly JM. Projection reconstruction techniques for reduction of motion effects in MRI. *Magn Reson Med*. 1992; 28(2):275–289. [PubMed: 1461126]
34. Deshmane A, Gulani V, Griswold MA, Seiberlich N. Parallel MR imaging. *J Magn Reson Imaging*. 2012 Jul; 36(1):55–72. DOI: 10.1002/jmri.23639 [PubMed: 22696125]
35. Edelman RR, Giri S, Pursnani A, Botelho MPF, Li W, Koktzoglou I. Breath-hold imaging of the coronary arteries using quiescent-interval slice-selective (QISS) magnetic resonance angiography: pilot study at 1.5 Tesla and 3 Tesla. *J Cardiovasc Magn Reson*. 2015 Nov.17:101. [PubMed: 26597281]
36. Kato S, Kitagawa K, Ishida N, et al. Assessment of coronary artery disease using magnetic resonance coronary angiography: a national multicenter trial. *J Am Coll Cardiol*. 2010 Sep 14; 56(12):983–91. DOI: 10.1016/j.jacc.2010.01.071 [PubMed: 20828652]
37. Lapner ST, Kearon C. Diagnosis and management of pulmonary embolism. *BMJ*. 2013 Feb 20.346:f757. doi: 10.1136/bmj.f757 [PubMed: 23427133]
38. Nagle SK, Schiebler ML, Repplinger MD, et al. Contrast enhanced pulmonary magnetic resonance angiography for pulmonary embolism: building a successful program. *Eur J Radiol*. 2016 Mar; 85(3):553–563. DOI: 10.1016/j.ejrad.2015.12.018 [PubMed: 26860667]
39. Edelman RR, Silvers RI, Thakrar KH, et al. Nonenhanced MR angiography of the pulmonary arteries using single-shot radial quiescent-interval slice-selective (QISS): a technical feasibility study. *J Cardiovasc Magn Reson*. 2017 Jun 30.19(1):48. doi: 10.1186/s12968-017-0365-3 [PubMed: 28662717]
40. Koktzoglou I, Murphy IG, Giri S, Edelman RR. Quiescent interval low angle shot magnetic resonance angiography of the extracranial carotid arteries. *Magn Reson Med*. 2016 May; 75(5): 2072–7. DOI: 10.1002/mrm.25791 [PubMed: 26072706]
41. Koktzoglou I, Edelman RR. Super-resolution intracranial quiescent interval slice-selective magnetic resonance angiography. *Magn Reson Med*. 2017 May 3. doi: 10.1002/mrm.26715
42. Akçakaya M, Hu P, Chuang ML, et al. Accelerated noncontrast-enhanced pulmonary vein MRA with distributed compressed sensing. *J Magn Reson Imaging*. 2011 May; 33(5):1248–55. DOI: 10.1002/jmri.22559 [PubMed: 21509886]

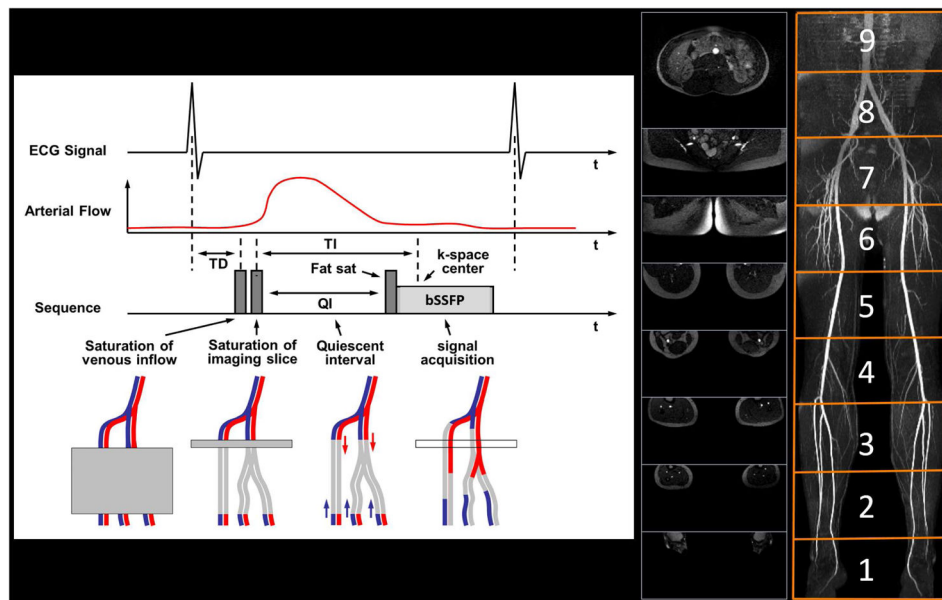


**Figure 1.**

QISS technique. Pulse sequence diagram for QISS MRA as configured for imaging of the peripheral arteries (left). In-plane saturation and tracking venous saturation radiofrequency (RF) pulses are applied approximately 100 ms after the R-wave to suppress non-arterial background signals. Following a preset quiescent interval (QI, ~200–300 ms), a fat-saturation RF pulse is applied to suppress the appearance of fat within the slice, followed by an  $\alpha/2$  preparation and a bSSFP readout (~300 ms) with a flip angle of  $\alpha$  (~90°). One slice is acquired per RR interval. In this example, 432 contiguous 3-mm thick slices were acquired as nine groups of 48 slices, with each group centred at the magnet isocentre to minimise off-resonance artefacts (middle). The images can be composed into projection angiograms (right).





**Figure 2.**

**An** 88-year-old man with claudication, type 2 diabetes, and cardiac arrhythmia. Left: CTA; right QISS MRA. The CTA was non-diagnostic due to the presence of extensive vascular calcifications; however, QISS MRA was completely unaffected by the vascular calcifications and demonstrated the patency of proximal vessels and occlusions of calf vessels.

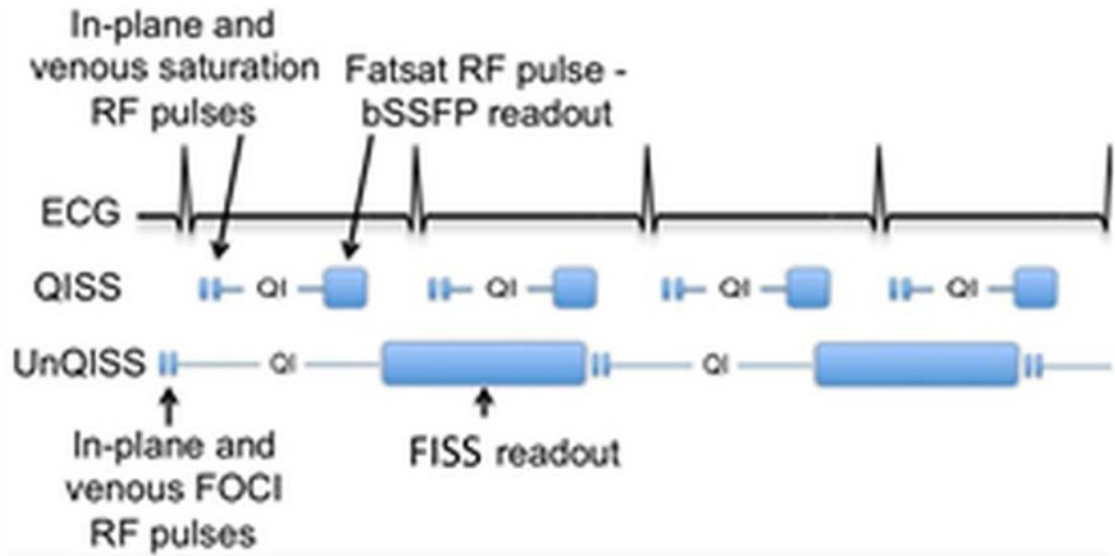


**Figure 3.**

Timing diagrams illustrating the differences between ECG-gated QISS MRA and UnQISS MRA. Compared with ECG-gated QISS MRA, UnQISS MRA is not synchronised to the cardiac cycle, uses frequency offset corrected inversion (FOCI) RF pulses instead of saturation pulses to suppress in-plane tissue and venous signals, much lengthier QI, and radial FISS readouts instead of Cartesian bSSFP readouts. Because FISS naturally suppresses fat signal, no fat-saturation pulses are needed.

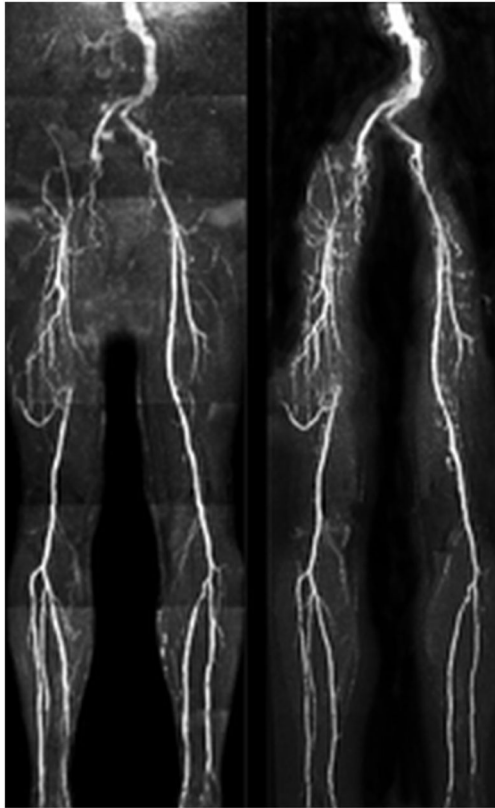


**Figure 4.** Patient with multi-focal PAD. Left: ECG-gated QISS. Right: UnQISS using a radial k-space trajectory. Occlusions of the right external iliac and superficial femoral arteries and collaterals are comparably shown by UnQISS and QISS, as is the occlusion of the left anterior tibial artery.

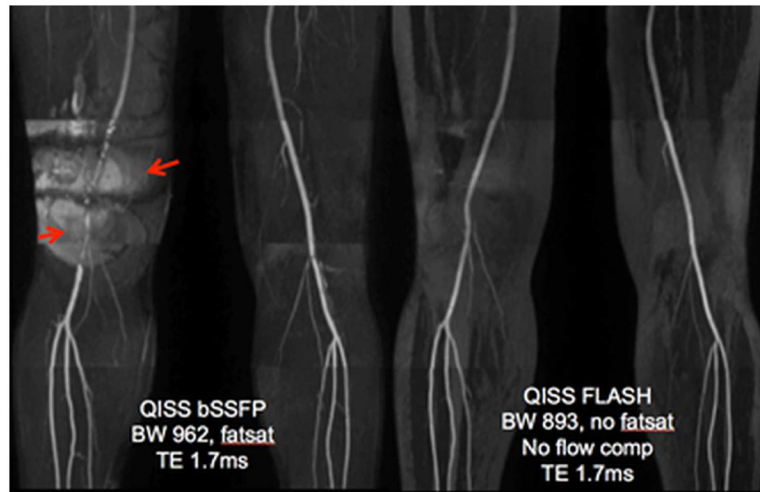


**Figure 5.** Healthy volunteer imaged at 3 T using QISS bSSFP (left) and QISS FLASH (right) protocols. The subject had a metal fixation rod in the right femur relating to a prior fracture. QISS FLASH shows much better image quality in the region of the metal rod. The right superficial femoral artery, which is completely obscured by magnetic susceptibility-related artefact (arrows) in the QISS bSSFP images, is well depicted in the QISS FLASH image.

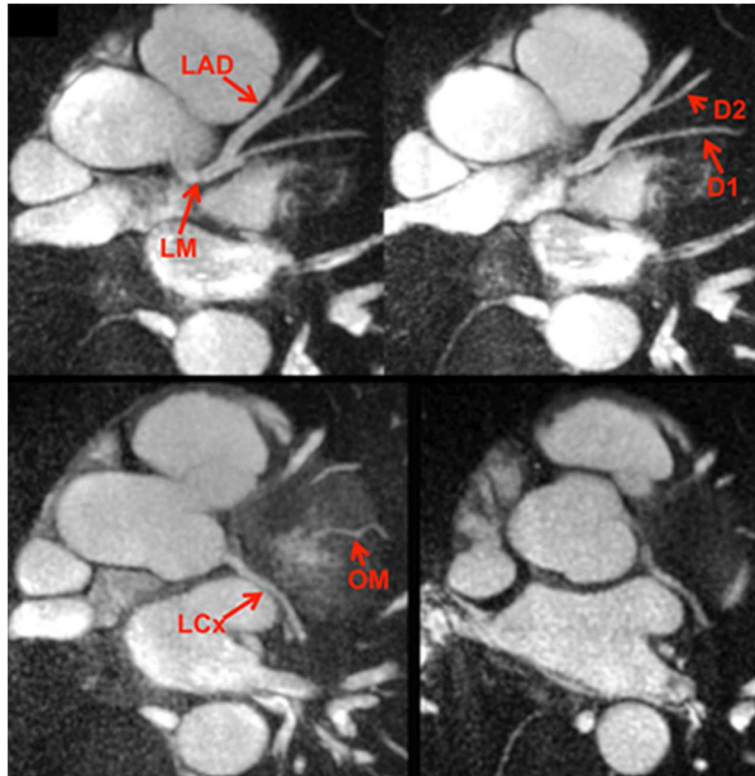


**Figure 6.** Examples of thin maximum intensity projections reconstructed from single breath-hold, two-shot radial QISS MRA of the coronary arteries in a healthy subject. LM, left main artery; LAD, left anterior descending artery; D1, first diagonal branch; D2, second diagonal branch; LCx, left circumflex artery; OM, obtuse marginal branch.

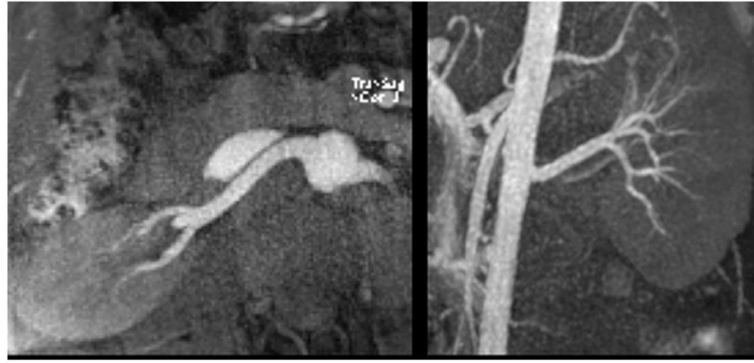


**Figure 7.** Maximum intensity projections from axial (left) and oblique coronal (right) single breath-hold, single-shot radial QISS MRA of the renal arteries. Images can be efficiently acquired in multiple imaging planes with near-isotropic spatial resolution.

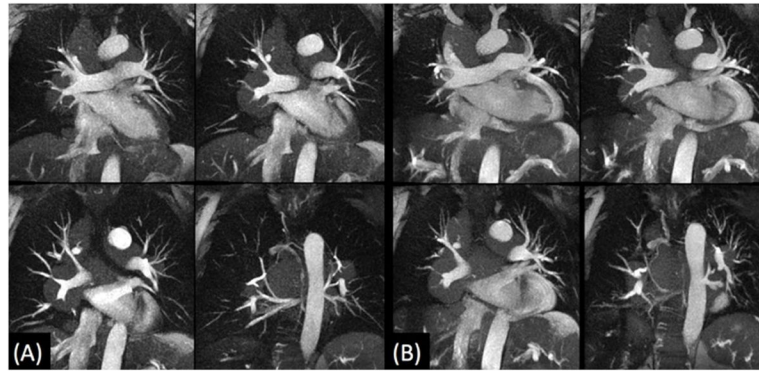


**Figure 8.** Breath-hold (a) and free-breathing navigator-gated (b) single-shot radial QISS MRA in a patient with pulmonary sarcoidosis. Aside from diaphragm position (end-inspiration (a), end-expiration for (b)), the techniques similarly show the pulmonary artery compression caused by extensive mediastinal lymphadenopathy.

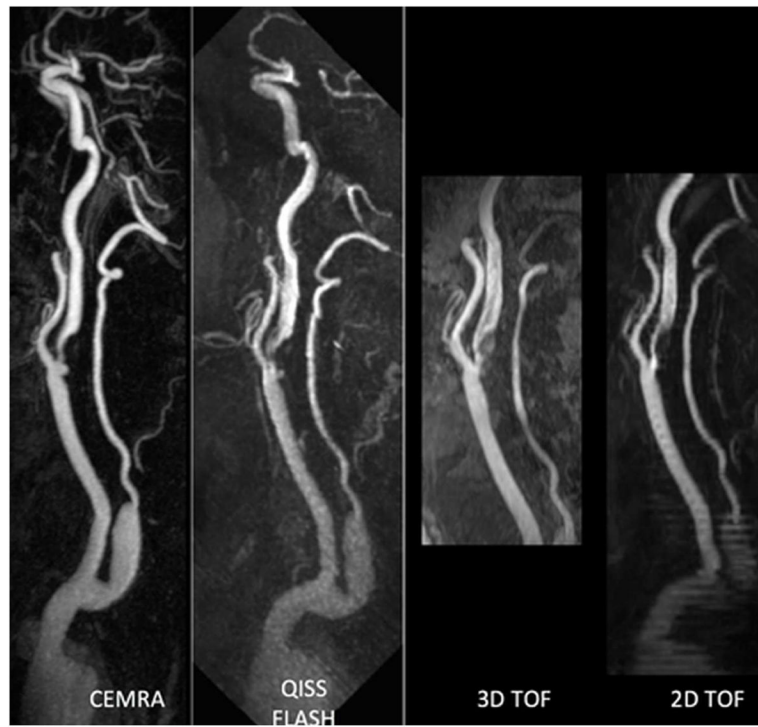


**Figure 9.** Patient with severe stenosis and ulceration of the proximal internal carotid artery and bulb. QISS FLASH shows the lesions comparably to CEMRA, with more extensive head-to-foot coverage and less artefact than either two-dimensional or 3D time-of-flight MRA.